Palladium Bisphosphine Mono-Oxide Complexes: Synthesis, Scope, Mechanism, and Catalytic Relevance

Shenghua Yang, Min Deng, Ryan A. Daley, Andrea Darù, William J. Wolf, David T. George, Senjie Ma, Bryn K. Werley, Erika Samolova, Jake B. Bailey, Milan Gembicky, Jonathan Marshall, Steven R. Wisniewski, Donna G Blackmond,* Keary M Engle*

ABSTRACT: Recent studies in transition metal catalysis employing chelating phosphines have suggested a role for partial ligand oxidation in formation of the catalytically active species, with potentially widespread relevance in a number of catalytic systems. We examine the internal redox reaction of Pd^{II}(bisphosphine)X_2 (X = Cl, OAc, *etc.*) complexes to reveal previously underexplored aspects of bisphosphine mono-oxides (BPMOs), including evaluation of ligand structure and development of general reaction conditions to access a collection of structurally diverse BPMO precatalysts based on organopalladium oxidative addition complexes. In particular, a series of Pd^{II}(BPMO)(R)(X) (R=Aryl, Alkyl; X=I, Br) oxidative addition complexes bearing 24 different BPMO ligands were characterized by NMR and X-ray crystallography. Comparison of the catalytic performance of the oxidative addition complexes of phosphine versus bisphosphine mono-oxides as precatalysts is demonstrated to be an enabling diagnostic tool in Pd catalytic reaction development. Finally, the differences in catalytic behavior between bisphosphine and bisphosphine mono-oxide complexes were rationalized through solid-state parametrization and stoichiometric experiments.

INTRODUCTION

Homogeneous transition metal catalysis is widely applied in the pharmaceutical, agrochemical, and fine chemical industries to produce functionally diverse organic small molecules.[1–3] Phosphine ligands are widely used in homogeneous catalysis, and over the past three decades, the scientific community has devoted intense efforts to the development of large screening libraries of mono- and bisphosphine ligands to promote a variety of catalytic reactions and to understand the mechanisms of these catalytic processes.[4–8] Nevertheless, in many cases, the structure of the *catalytically active* metal–ligand species, arguably the most crucial piece of information, remains poorly understood. This knowledge gap hampers rational catalyst development, slows the pace of research, and gives rise to irreproducibility issues across the chemical community.

The use of bisphosphine ligands in catalysis dates to Kagan's report of the chiral ligand DIOP for asymmetric rhodium-catalyzed hydrogenation.[9,10] In the realm of Pd^0-catalyzed C–C cross-coupling, chelating bisphosphine ligands were initially reported to be ineffective in early studies of Mizoroki–Heck reactions[11] but have subsequently played an important role in both stereoselective and non-stereoselective transformations (Scheme 1). In 1979, Kumada found that dppf increased product yield and decreased competitive chain-walking processes compared to PPh_3 in the cross-coupling of a secondary alkyl Grignard reagent and organohalides.[12] Seminal reports by Shibasaki and Overman in 1989 then disclosed the first examples of asymmetric intramolecular Heck cyclizations with (*R*)-BINAP and (*R,R*)-DIOP, respectively, in which a cationic pathway could account for the success of bisphosphine ligands.[13–15] In the field of C–N coupling, Buchwald and Hartwig showed separately that bisphosphines ligands also play a beneficial role, including expansion of substrate scope, suppression of side reactions, and ability to use milder reaction conditions.[16–18] Bisphosphine ligands have also been used to great effect in Suzuki–Miyaura, Stille, and Negishi couplings; α-arylations of carbonyl compounds; allylic substitutions; and other widely used Pd^0-catalyzed reactions.[2] While extensive efforts have been devoted to mapping ligand effects in Pd^0-catalyzed coupling reactions, key questions regarding catalyst speciation and the importance of bidentate coordination versus monodentate coordination in different systems remain unresolved.[15]

Scheme 1: Early examples of chelating bisphosphine ligands in Pd⁰-catalyzed C–C and C–N cross-coupling.

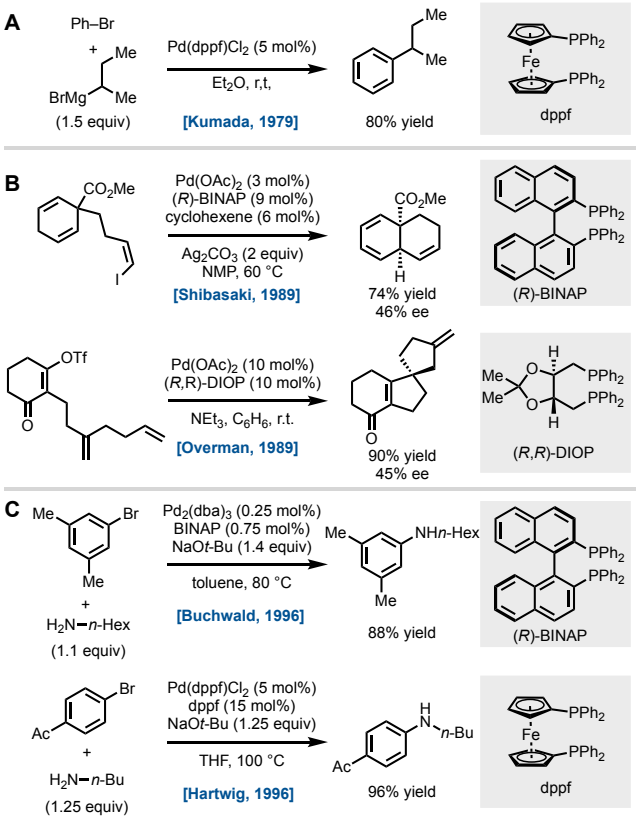

These and other related palladium-catalyzed coupling reactions begin with initial generation of the active form of the catalyst, typically from a Pd^{II} or a Pd^0 precursor and the bisphosphine ligand combined in situ or alternatively from a well-defined pre-ligated pre-catalyst.[19] When Pd^{II} salts are used, a common catalytic activation for simple phosphine ligands[20–22] involves an internal redox reaction (i.e., disproportionation) that produces Pd^0 and generates the corresponding bisphosphine mono-oxide (BPMO) of the bisphosphine ligand. BPMOs are classically considered to be mere byproducts in such contexts,[23] although the value of independently prepared BPMOs as unique ligands in transition metal catalysis has been established through important contributions of Grushin and others.[24] Notably Grushin and Yang have independently developed elegant catalytic methods for preparing BPMOs derived from triaryl and diarylalkyl bisphosphines.[25]

Our interest in understanding the role of phosphine oxidation in catalyst activation and speciation stems from our previous finding that a bisphosphine ligand, Xantphos, was the most effective from a screen of >30 ligands during the optimization of a Pd^0-catalyzed direct C–H arylation of azaheterocycles with heteroaryl bromides.[26] Initially, this observation was puzzling as bidentate binding of the ligand would prevent coordination of the pivalate base needed for the key concerted metalation/deprotonation (CMD) step, supported by the observation that addition of excess Xantphos completely inhibited catalysis. Eventually, kinetic, structural, and computational data revealed that in-situ oxidation of Xantphos to Xantphos(O) was responsible for catalyst activation (Scheme 2A). In particular, the hemilabile nature of the phosphine oxide arm allows for binding of the pivalate base to promote CMD. Related work by other groups has since implicated involvement of in situ generated BPMOs in diverse Pd^0-catalyzed C–C and C–N bond-forming reactions with bisphosphine precursors, including QuinoxP*, DPEphos, dppBz, and (*R*)-BINAP.[27–32] The present work focuses on aspects of Pd^0(BPMO) generation and its relevance to catalysis that remain underexplored (Scheme 2B). Unresolved questions include: (1) With which bisphosphine ligands and under which conditions does in situ oxidation take place? (2) What are the consequences of in situ oxidation on active catalyst structure and reactivity? (3) What role does the metal-to-ligand ratio play in the formation of the active catalyst? Herein, we apply a combination of organometallic synthesis, X-ray crystallography, and reaction kinetics to shed light on these questions and other aspects of BPMO ligands and their role in palladium catalysis.

Scheme 2: Early examples of chelating bisphosphine ligands in Pd^0-catalyzed C–C and C–N cross-coupling.

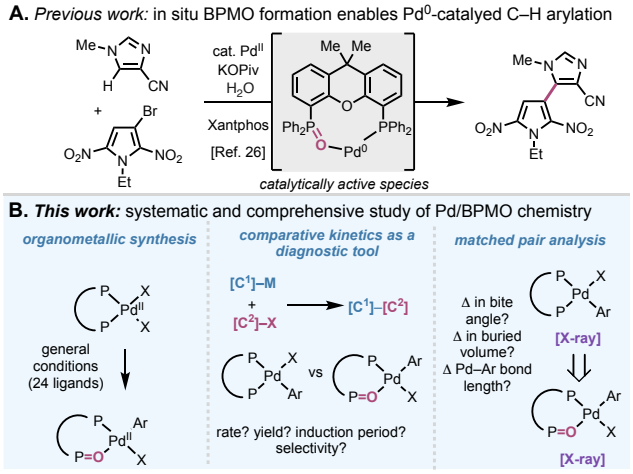

RESULTS AND DISCUSSION

A central challenge in the early stages of this study was to identify well-defined Pd(BPMO) complexes with the ligand in a clearly specified mono-oxidized state and with other enabling features. First, the complex should combine stability under ambient conditions with catalytic potency. Additionally, the complexes should be simple to prepare, ideally using the parent bisphosphine directly without independent synthesis of the BPMO,[25] which can require tedious separation and purification on larger scale. Finally, we chose systems where the non-oxidized Pd(bisphosphine) counterpart is available, allowing for side-by-side comparison of the structure and reactivity of Pd(BPMO) and Pd(bisphosphine) "matched pairs" that are structurally identical except for the oxidation state of the ligand.

Optimization of synthetic method towards Pd^{II}(BPMO)(R)(X) complexes

In pilot studies, we determined that Pd^0(BPMO)•L_n adducts with various capping ligands were insufficiently stable and long-lived for these purposes (see Supporting Information). We thus turned attention to Pd^{II}(BPMO)(R)(X) oxidative addition complexes as candidates. In addition to being single-component and stable complexes in many cases,

$Pd^{II}(L_n)(R)(X)$ oxidative addition complexes are commonly used as well-defined precatalysts;[19,33] we anticipated that Pd^{II}(BPMO)(R)(X) oxidative addition complexes could likewise be directly employed in catalysis. While previous studies have successfully prepared individual Pd^{II}(BPMO)(R)(X) oxidative addition complexes from the corresponding bisphosphines or independently synthesized BPMOs,[22,26–29] a generally applicable procedure that encompasses a variety of BPMOs is lacking.

We initiated our experimental work by developing a robust and high-yielding protocol for tandem bisphosphine oxidation and in situ trapping with an aryl iodide electrophile using (*S*)-BINAP (**L1**) as the model ligand. After some experimentation, we identified optimal conditions by adapting literature methods;[27,28] in our standard procedure: aqueous KOH solution (1M, 5 equiv KOH) is added into a pre-stirred mixture of $Pd(OAc)_2$, **L1**, and 4-CN-C_6H_4I at room temperature for 30 min to furnish oxidative addition complex **1a** in 92% ^{1}H NMR yield (68% isolated by recrystallization, entry 1). The structure of **1a** was unambiguously assigned by single-crystal X-ray diffraction. In the solid state **L1(O)** coordinates through κ^2-P(III),P(V)=O binding. Additionally, by ^{31}P NMR spectroscopy, ^{31}P–^{31}P coupling is absent, and the P^V=O resonance of **1a** is downfield compared to that of the free bisphosphine mono-oxide ligand (BINAP(O), **L1(O)**), indicating that **L1(O)** also coordinates through a κ^2 mode in solution. Key observations from our optimization experiments are summarized in Table 1. In the absence of KOH, the product could not be detected (entry 2), demonstrating the importance of base in enabling the reaction. Additionally, when KOH was added as a solid without water, the transformation was sluggish even at extended reaction time (16 h), pointing to the possibility of the reaction being mass-transfer-limited under these conditions (entry 3). Weaker inorganic bases, such as K_3PO_4, K_2CO_3, and $KHCO_3$ were also effective (entries 4–6). In the case of K_3PO_4, the reaction proceeded at room temperature as in the case of KOH, whereas with K_2CO_3 and $KHCO_3$, heating the biphasic mixture to 80 °C improved conversion. The soluble organic base, Et_3N, was also effective but gave 19% lower yield compared to KOH (entry 7).

Alternative palladium(II) salts beyond $Pd(OAc)_2$ were also investigated. While both $Pd(OAc)_2$ and $PdCl_2$ have been previously shown to participate in mono-oxidation, the reactivity of other Pd(II) salts commonly used in catalysis remains unknown. We found that $Pd(TFA)_2$ is as effective as $Pd(OAc)_2$ (entry 8). Simple PdX_2 salts (X = Cl or Br) benefit from pre-ligation to the bisphosphine due to poor solubility of the parent palladium salts in toluene (entries 9 and 10). The effect is particularly pronounced with $PdBr_2$, which was insoluble and did not coordinate to the ligand but reacted smoothly when pre-ligated (entry 11). A variety of solvents spanning different dielectric constants and water miscibility, such as DCM, THF, and MeCN, were well tolerated (entries 12–14).

Table 1. Optimization of tandem bisphosphine oxidation / oxidative addition protocol.[a]

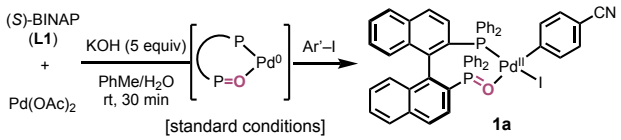

entry	deviation from standard conditions[a]	% yield (**1a**)[b]
1	(none)	92% (68%)[c]
2	no KOH, 16 h	n.d.
3	KOH (solid), without added H_2O, 18 h	26%
4	K_3PO_4 instead of KOH	85%
5	$KHCO_3$ instead of KOH	20% [96%][d]
6	K_2CO_3 instead of KOH	23% [86%][d,e]
7	Et_3N instead of KOH	73%
8	$Pd(TFA)_2$ instead of $Pd(OAc)_2$	98%
9	$PdCl_2$ instead of $Pd(OAc)_2$, no prestirring	13%[e]
10	pre-ligated (**L1**)$PdCl_2$	85%
11	pre-ligated (**L1**)$PdBr_2$	83%
12	THF instead of PhMe	95%
13	DCM instead of PhMe	88%
14	MeCN instead of PhMe	88%

a Reaction conditions **L1** (0.1 mmol), Pd(OAc) (0.1 mmol), 4-CN-C_6H_4I (0.2 mmol), KOH (aq., 1.0 M, 5 equiv), PhMe (0.04 M); see Supporting Information for experimental details. *b* Yields determined by ^{31}P NMR analysis of the crude reaction mixture using triphenylphosphate as the internal standard. *c* Values in parentheses correspond to isolated yields via precipitation. *d* Values in brackets correspond to reactions performed at 80 °C, 30–50 min. *e* (*R*)-BINAP was used instead of (*S*)-BINAP.

The trapping abilities of various organohalide electrophiles were next evaluated (Table 2). Electron-deficient, -neutral, or -rich aryl iodides all reacted efficiently to yield the corresponding Pd(**L1**(O))(Ar)(I) complexes **1b**–**1h**. Interestingly, methyl iodide also reacts competently, though in this case higher loading of the electrophile was required (**1j**). Beyond organoiodides, aryl bromides also react competently, as exemplified by **1k**. In these cases, however, analysis of crude mixture is complicated by extensive Br-to-OH (or Br-to-OAc) ligand exchange under the reaction conditions. Alternative aryl electrophiles, such as triflates and chlorides, gave little conversion at room temperature. Complexes **1b**, **1e**, **1f**, **1g**, **1h**, **1i** and **1j** were crystallized and characterized by X-ray diffraction. In all of the structures, the aryl group is positioned *trans* with respect to the oxidized phosphorus atom, demonstrating the stronger *trans* influence of the non-oxidized phosphorus atom compared to the phosphine oxide.

Table 2. Scope of electrophilic trapping reagents

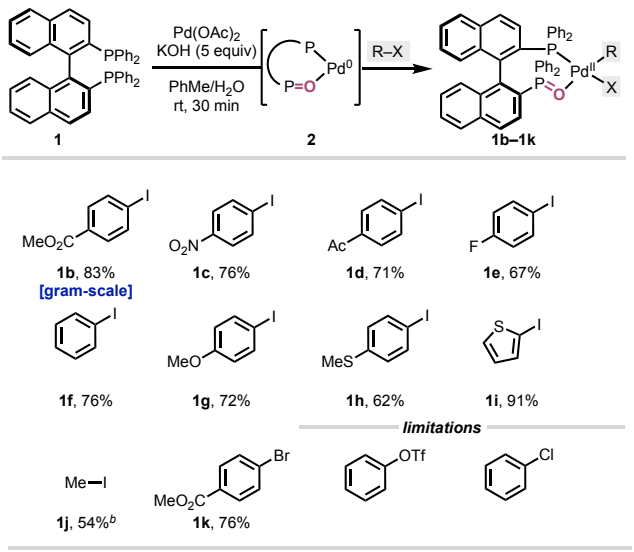

a Reaction conditions: **1** (0.2 mmol), **2** (0.2 mmol), **3** (1.15 equiv), KOH (1.0 M aqueous solution, 5eq), Toluene (0.02–0.05 M), rt, 1h. Values correspond to isolated yields. *b* MeI (5.0 equiv), KOH (3.0 equiv).

Scope of bisphosphine ligands and organohalides

Next, we evaluated the scope of bisphosphine ligands that participate in this in situ bisphosphine oxidation–trapping protocol, focusing on systematically varying the backbone structure as well as the substituents on phosphorous (Table 3). Previous reports on bisphosphine oxidation have generally focused on a single ligand relevant to a catalytic transformation of interest.[26–32] A comprehensive study of different ligand classes under standardized conditions is lacking, so the structural requirements for in situ oxidation remain poorly understood. We chose 4-CO_2Me-C_6H_4I as the standard trapping reagent for these experiments because the corresponding oxidative addition complexes possess a diagnostic ^{1}H NMR signal (ca. 3.8 ppm, Ar-CO_2CH_3) and exhibit generally desirable solubility profiles.[33]

Ligands derived from biphenyl backbones were first examined and were found to react efficiently in the in situ mono-oxidation/trapping sequence. Within the BINAP **(L1–L3**) and SEGPHOS (**L4**–**L6**) families, increased steric encumbrance on the phosphorous was tolerated, and in all cases, the corresponding bisphosphine mono-oxide oxidative addition complexes can be isolated in good to excellent yields. (*R*)-H_8-BINAP (**L7**), BIPHEP (**L8**), and MeO-BIPHEP (**L9**, **L10**) ligands all reacted smoothly. With some of these ligands, performing the reaction in THF instead of toluene is critical for obtaining high yield, presumably due to sluggish coordination of the bisphosphine ligand to $Pd(OAc)_2$ in toluene at room temperature. Spiro bisphosphines have recently emerged as powerful ligands in asymmetric catalysis.[35] To our delight, (*S*)-SDP (**L11**) reacted smoothly in THF to give **L11**(O)-ligated oxidative addition complex, as confirmed by X-ray crystallography. Notably, SDP mono-oxide ligands (e.g., **L11**(O)) have been shown by Zhou to enable highly enantioselective Mizoroki–Heck arylation.[36,37]

Wide-bite-angle Xantphos ligands capable of adopting *trans*-spanning coordination modes, **L12** and **L13**, both reacted efficiently. Interestingly, in the corresponding oxidative addition complexes, both bisphosphine mono-oxides, Ph-Xantphos(O) and Cy-Xantphos(O), coordinate in a *cis* fashion. A series of bisphosphines based on the *o*-phenylene backbone containing alkyl and (hetero)aryl substituents on phosphorous with different steric and electronic properties were next considered. All ligands reacted smoothly in DCM. Alkyl (**L14**, **L15**), aryl (**L16–L18**), and heteroaryl (**L19**) substitutions on phosphorus atoms are well-tolerated, and oxidative addition complexes derived from **L15–L19** were characterized by X-ray crystallography.

Table 3. Scope of bisphosphine ligands and selected X-ray structures. (Solvent molecules and disorder are omitted for clarity).

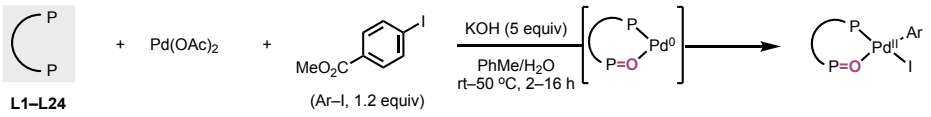

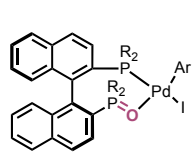

L1 (R = Ph): 80%
L2 (R = 4-Tol): 89% [X-ray]
L3 (R = 3,5-Xyl): 65%[b,c]

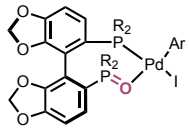

L4 (R = Ph): 82%[b]
L5 (R = 3,5-Xyl): 80% [76%] [X-ray][b,c,d]
L6 (R = DTBM-Ph): 82%

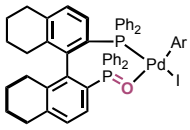

L7: 77%[b]

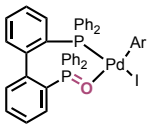

L8: 61% [X-ray]

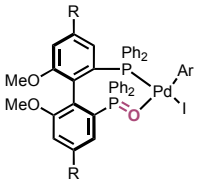

L9 (R=H): 60% [X-ray][e]
L10 (R=OMe): 90% [82%] [X-ray][f]

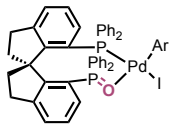

L11: 71% [X-ray][b,e]

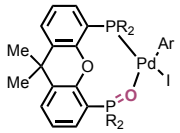

L12 (R = Ph): 60% [X-ray]
L13 (R = Cy): 61% [X-ray]

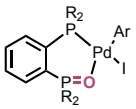

L14 (R = ^{i}Pr): 50%[g]
L15 (R=Cy): 51% [X-ray][g]
L16 (R = Ph): 76% [X-ray][g]
L17 (R = 4-F-C_6H_4): 58% [X-ray][g]
L18 (R = 4-OMe-C_6H_4): 75% [X-ray][g]
L19 (R = 2-furyl): 39% [X-ray][g]

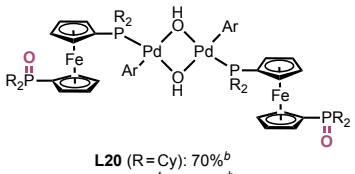

L20 (R = Cy): 70%[b]
L21 (R = ^{t}Bu): 61%[b]
L22 (R = ^{i}Pr): 63% [X-ray][b]

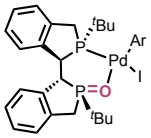

L23: 52% [X-ray]

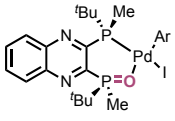

L24: 79% [X-ray]

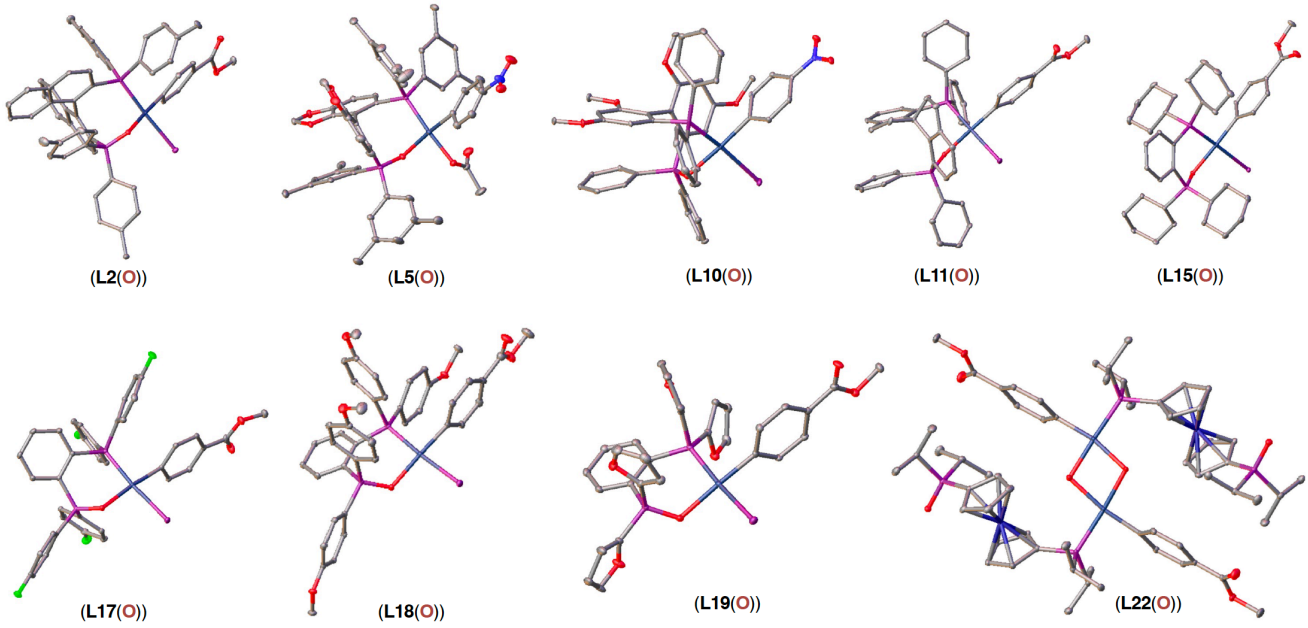

[a] Reaction conditions **L1**–**L24** (0.1–0.2 mmol), $Pd(OAc)_2$ (1 equiv), 4-CO_2Me-C_6H_4I (1.2 equiv), KOH (aq., 1.0 M, 5 equiv), PhMe (0.02–0.05 M), rt–50 °C; see Supporting Information for experimental details. [b] THF instead of PhMe. [c] The (*R*) enantiomer of the ligand was used. [d] Value in brackets corresponds to reaction with 4-NO_2-C_6H_4I followed by AgOAc in place of 4-CO_2Me-C_6H_4I; X-ray structure of the NO_2 complex with acetate instead of iodide was obtained. [e] Isolated yield obtained with (*S*) enantiomer as drawn; X-ray structure obtained with (*R*) enantiomer from an independent experiment. [f] Value in brackets corresponds to reaction with 4-NO_2-C_6H_4I in place of 4-CO_2Me-C_6H_4I; X-ray structure of the NO_2 complex was obtained. [g] DCM instead of PhMe.

For the 1,1'-bis(phosphino)ferrocenes, the parent ligand dppf, which contains diphenylphosphino groups, led to an intractable product mixture (Scheme 3, see Supporting Information for details). More strongly σ-donating dialkylphosphino variants furnished oxidative addition

complexes as a mixture of palladium iodides and μ-OH dimers when the standard trapping electrophile, 4-CO_2Me-C_6H_4-I, was used. Gratifyingly, the μ-OH dimers could be cleanly obtained as the major product when 4-CO_2Me-C_6H_4-Br was used instead (**L20–L22**). These dimers are characterized by their diagnostic ^{1}H NMR signal at -0.5 ppm ($CDCl_3$). Furthermore, the solid-state structure of the dimer bearing **L22**(O) was established by X-ray crystallography. Chiral-at-phosphorus ligands are not only useful in asymmetric catalysis but also serve the dual purpose of providing mechanistic insight into the operative pathway for phosphine oxidation based on whether P=O bond formation is stereoretentive or invertive (vide infra). Both (1*R*,1'*R*,2*S*,2'*S*)-Duanphos (**L23**) and (*R*,*R*)-QuinoxP* (**L24**) ligands reacted smoothly. X-ray crystal structures of both bisphosphine mono-oxide oxidative addition complexes establish that the oxygen is inserted into the same face of phosphine coordination. These observations agree with seminal early studies by Grushin with chiral-at-P monophosphines[21] and by more recent studies with (*R*,*R*)-QuinoxP by Ji and colleagues.[25]

Some limitations in the scope of this method merit discussion. In addition to dppf, bisphosphine ligands with flexible backbones, including DPEphos and dppe, gave evidence of in situ ligand oxidation but led to intractable mixtures, potentially because of the weakly coordinating nature of the BPMO ligand (see Supporting Information).

Scheme 3: Flexible bisphosphine ligands that lead to intractable product mixtures

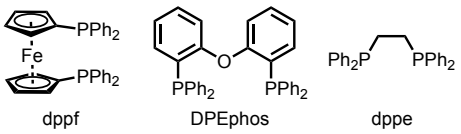

Isotope labeling

To gain insight into the origin of the oxygen atom in the BPMO product, we performed a series of isotope labeling experiments using BINAP (L1) as a model ligand (Scheme 4, top). When pre-ligated complex Pd^{II}(BINAP)$(OAc)_2$ was treated with K^{18}OH (1.0 M in $H_2{}^{18}O$, >98% ^{18}O) under air with conditions otherwise analogous to those shown in Table 1, quantitative transfer of the ^{18}O label to the product, Pd(L1(^{18}O))(Ar)(I), was detected by HRMS analysis (see Supporting Information for details), showing no evidence of competitive ^{16}O incorporation from the acetate ligands or O_2 in the air. When a similar experiment was performed with chloride-containing starting complex, Pd^{II}(BINAP)Cl_2, equally high ^{18}O incorporation was detected (see Supporting Information). Control experiments with K^{16}OH showed complete transfer of the ^{16}O label. (see Supporting Information). The isotope labeling data are consistent with inner- or outer-sphere hydroxide anion as the oxygen atom source in BPMO formation. Between these two possibilities, the data above showing stereoretentive P–O bond formation with chiral-at-P ligands L23 and L24,[21,25] is consistent with inner-sphere P–O bond formation (Scheme 4, bottom).

Previously Hayashi performed an experiment in which $H_2{}^{18}O$ Et_3N, $Pd(OAc)_2$, and BINAP were combined in benzene, and the ^{18}O:^{16}O ratio of thusly formed BINAP(O) was measured at several time points and found to increase over time.[22] The authors rationalized this result by invoking OAc^- as the oxygen atom source in BINAP(O) formation, which becomes enriched in ^{18}O as the reaction progresses. In light of the data above, however, an alternative interpretation of Hayashi's data is a scenario involving competitive OAc^- versus OH^- pathways at low [OH^-] concentration.

Scheme 4: ^{18}O-Labeling reveals source of O-atom in BINAP(O) to be hydroxide.

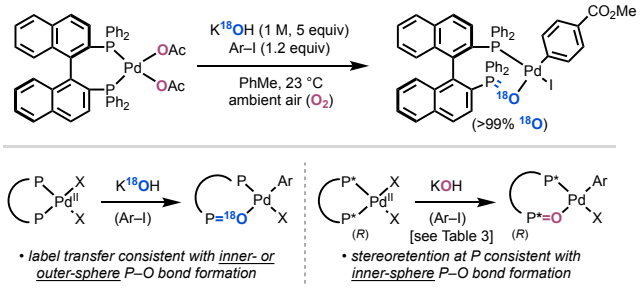

Kinetics of bisphosphine oxidation

We developed a protocol for monitoring BPMO formation by React-IR that takes advantage of the trapping strategy described above. Kinetic profiles of the reaction using BINAP **L1** as ligand are shown in Figure 1. The reaction is found to be zero-order with respect to aryl iodide concentration, consistent with the notion that oxidative addition of the aryl iodide to Pd^0(BINAP(O)) is not rate-limiting and that Ar-I serves as a trap of the transient Pd^0(BPMO) complex. Increase in Pd or KOH concentrations enhances the rate. The fact that higher [KOH] gives similar rates as higher [Pd] supports the role of KOH in phosphine oxidation, potentially by driving the equilibrium towards formation of the reactive Pd^{II}(BINAP)(OH)(X) intermediate depicted in Scheme 4. Figure 2 compares kinetic profiles for the reaction using different phosphine ligands, showing fairly robust reactions with some differences in rates under identical standard conditions.

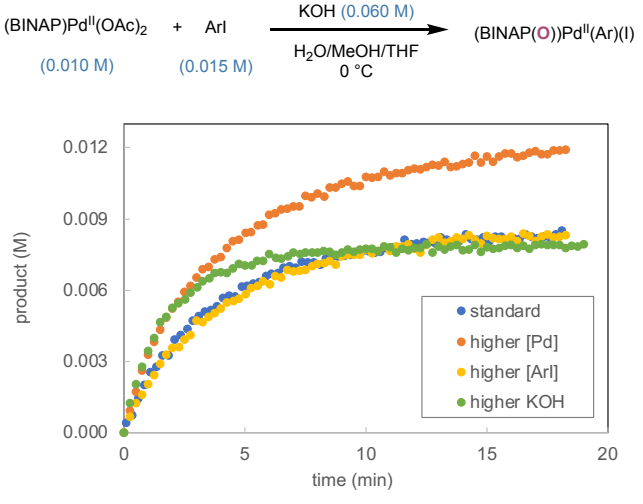

Figure 1. Kinetics of BINAP oxidation monitored by ReactIR.

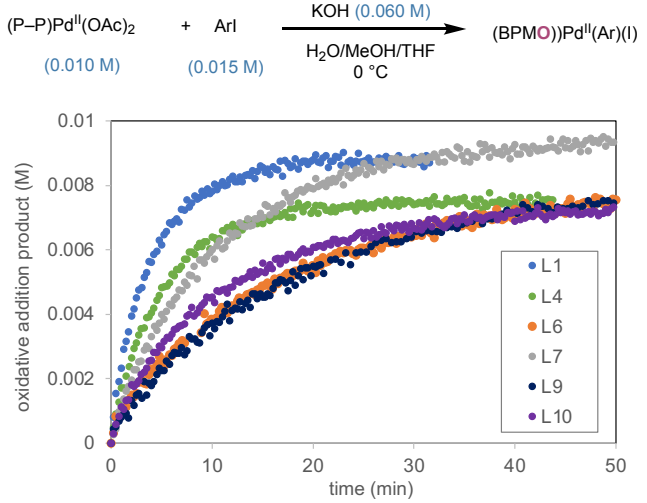

Figure 2. Comparative kinetics of the formation of BPMO oxidative addition complexes of different ligands.

Diagnosis of catalyst activation/deactivation

The broad library of BPMO oxidative addition complexes made available by the synthetic method described above presents the opportunity to diagnose various palladium catalyzed reactions by comparing kinetic profiles and overall yield of reactions to probe the effectiveness of Pd oxidative addition complexes with either bisphosphine or bisphosphine oxide as the precatalyst. We anticipate that reactions will belong to one of four general types (Types A–D, Scheme 5). In Type A reactions, both the bisphosphine and BPMO precatalysts will lead to comparable kinetics and product yields, indicating a catalytic reaction that is impartial to the oxidation state of the bisphosphine, suggesting a process in which many structurally distinct ligands can be employed interchangeably. In Type B reactions, on the other hand, the non-oxidized bisphosphine ligand exhibits more efficient catalysis, suggesting that in situ oxidation is a catalyst deactivation pathway. Type C reactions exhibit the opposite behavior to Type B, in which the pre-oxidized BPMO-containing precatalysts react with superior kinetics and turnover efficiency, suggesting that BPMO formation is a catalyst activation pathway. Lastly, in Type D reactions, neither type of precatalysts can recapitulate the reactivity of the as-described protocol, suggesting an alternative species is responsible for the observed reactivity. Below we provide several case studies of this workflow—both in the context of well-studied examples from the literature and previously unexamined reactions systems—and discuss mechanistic rationalization of the outcomes observed.

Scheme 5. Use of matched pairs as a diagnostic tool for catalyst activation/deactivation.

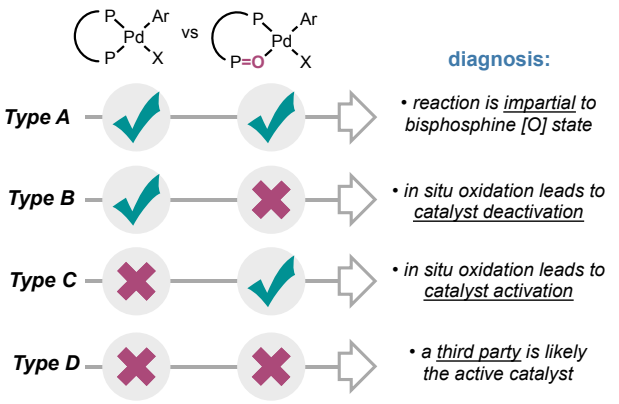

We first considered an unhindered Suzuki–Miyaura cross-coupling reaction between 3-F-C_6H_4Br and 4-OMe-$C_6H_4B(OH)_2$. While both oxidative addition complexes of BINAP and BINAP(O) are effective, little behavioral divergence was noted (Figure 6). The data suggest that BINAP and BINAP(O) are competent supporting ligands for this Suzuki–Miyaura cross coupling, making it a Type A system. This result reflects the robust nature of Suzuki–Miyaura cross-coupling, and its ability to be promoted by numerous different phosphine ligands (and ligand-free conditions), particularly in the unhindered system studied here. Care should be taken to not over-generalize this result to all Suzuki–Miyaura couplings, as BPMOs have previously been found to play a decisive role in atroposelective variants.[29]

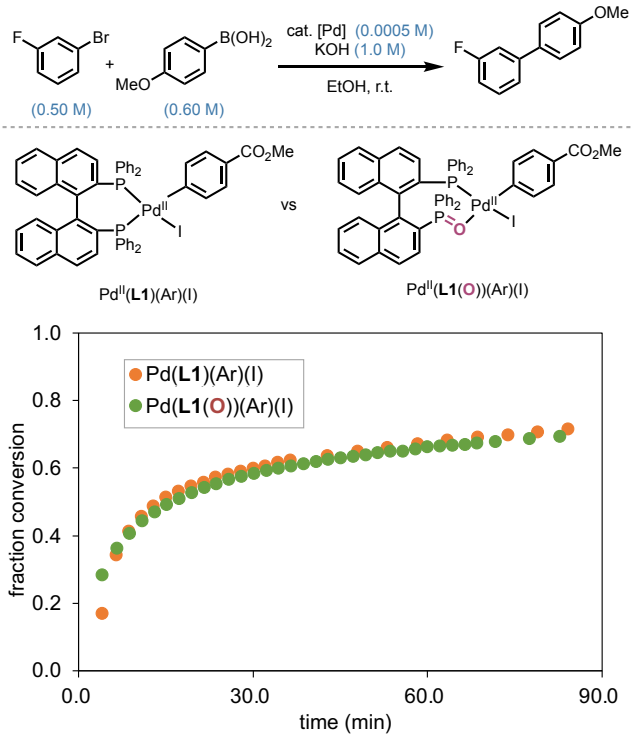

Figure 4. Comparison of Suzuki–Miyaura coupling reactions using Pd precatalysts developed from **L1** (orange symbols) or **L1** mono-oxide (green symbols) (Type A).

We next applied this workflow to two reaction systems previously studied by our research groups where a general mechanistic understanding is already in place. In a model Buchwald–Hartwig C–N coupling of 3-CF_3-C_6H_4Br and *n*-HexNH_2, catalyzed by BINAP-ligated palladium, which has been previously considered to operate with the non-oxidized bisphosphine as the active form (Figure 5).[38,39] we found that the Pd^{II}(BINAP)(Ar)(I) precatalyst reacted rapidly, with a rate exceeding the standard Pd^{II}(BINAP)$(OAc)_2$ precatalyst and also led to high final conversion. In contrast, the matched-pair Pd^{II}(BINAP(O))(Ar)(I) precatalyst was ineffective, yielding 5% of the desired C–N coupled product, even when the catalyst loading was tripled. In a separated stoichiometric experiment treatment of Pd^{II}(BINAP(O))(Ar)(I) with excess *n*-HexNH_2 led to quantitative formation for free BINAP(O) as monitored by ^{31}P NMR, suggesting facile displacement of the BPMO by the primary amine in this system (see Supporting Information). These data are consistent with a Type B reaction system, in which bisphosphine oxidation is expected to be a catalyst deactivation pathway. The possible role of BPMOs in other C–N coupling reactions with diverse amine and aryl (pseudo)halide coupling partners under different reaction conditions is a topic of ongoing investigation in our laboratories.

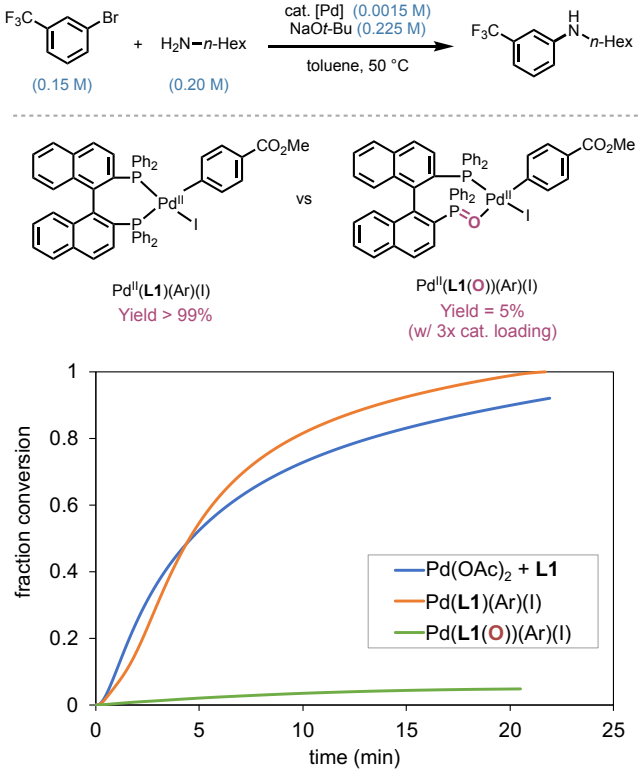

Figure 5. Reaction progress of a representative Buchwald–Hartwig amination of primary amines (Type B).

We then turned attention to a C–H arylation reaction between an electron-deficient imidazole and an aryl bromide catalyzed by palladium with Xantphos as the ligand (Figure 6). As discussed in the Introduction, prior mechanistic investigations have shown that this system requires in situ oxidation to Xantphos(O) for the reaction to proceed efficiently.[25] Indeed, consistent with expectations, we found that Pd^{II}(Xantphos(O))(Ar)(I), Pd^{II}(Xantphos(O))(Ar)(OPiv), and Pd^{II}(Xantphos)Cl_2 provided similar reaction profiles, whereas Pd^{II}(Xantphos)(Ar)(I) failed to deliver appreciable amounts of product. Collectively this data is consistent with a Type C reaction system with Xantphos(O) as the active form of the catalyst, where the induction period with Xantphos arises from an initial in situ oxidation prior to catalytic turnover.

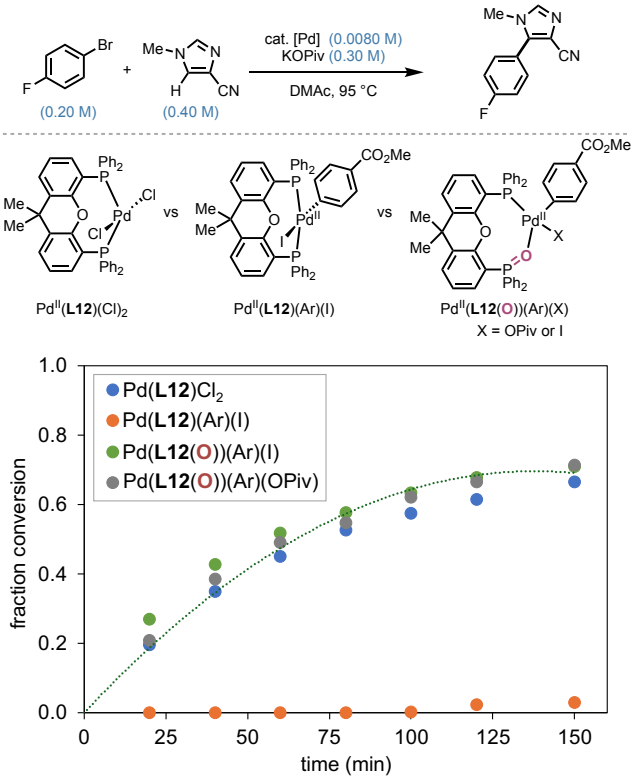

Figure 6. Model C–H arylation of imidazoles (Type C). Trend lines are added to guide the eye.

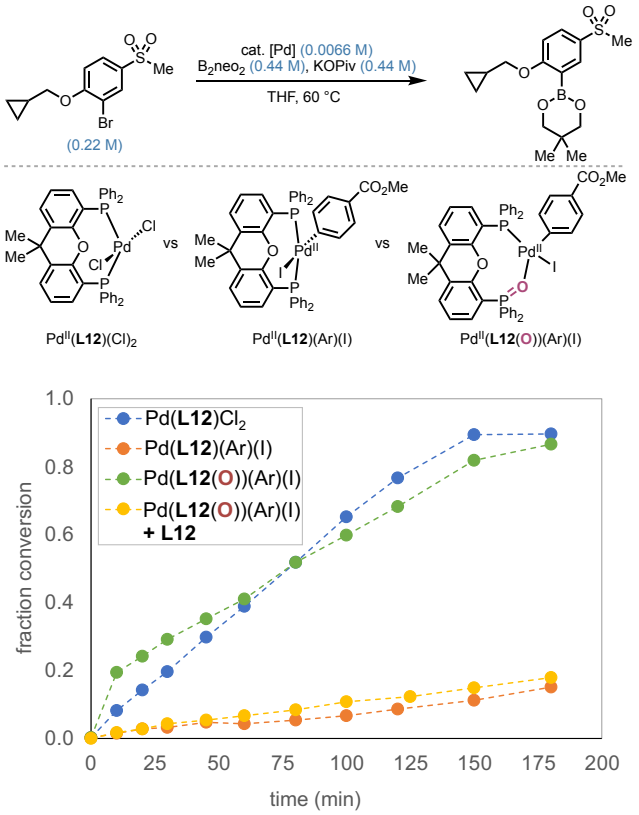

Figure 7. Model Miyaura borylation (Type C). Trend lines are added to guide the eye.

Finally, we applied this workflow to a Miyaura borylation of a pharmaceutically relevant aryl bromide which is used for the synthesis of a BET inhibitor (BMS-986378) (Figure 7).[40] The borylation with Pd^{II}(Xantphos(O))(Ar)(I) was found to proceed with the fastest initial rate. Furthermore, a greater than 10-fold difference in initial and overall kinetics was observed between reactions performed with Pd^{II}(Xantphos(O))(Ar)(I) and Pd^{II}(Xantphos)(Ar)(I) as the precatalyst, respectively. On the other hand, the reactions proceeded with similar overall rates with Pd^{II}(Xantphos)Cl_2 and Pd^{II}(Xantphos(O))(Ar)(I) as the precatalyst. These results suggest that 1) Pd complex containing Xantphos(O) as the ligand is a more effective catalyst for this borylation compared to that containing Xantphos as the ligand and 2) rapid in-situ oxidation of the Xantphos ligand occurs to generate the more active Pd BPMO catalyst when Pd^{II}(Xantphos)Cl_2 is used as the precatalyst. The data overall support the classification of this Miyaura borylation as a Type C reaction system where Pd catalyst ligated with Xantphos(O) is the more active form of the catalyst.

Matched-pair analysis

To understand the differences in catalytic behavior that arise from in situ bisphosphine mono-oxidation, we analyzed the solid-state structures of oxidized and non-oxidized "matched pairs", that is, oxidative addition complexes where the only difference is the presence or absence of the oxygen atom in question (Scheme 6). For this comparison, a series of bisphosphine palladium oxidative addition complex were synthesized, crystallized, and subjected to X-ray diffraction studies (see Supporting Information for details). This analysis includes seven previously unreported non-oxidized bisphosphine oxidative addition complexes, and one previously reported example from the literature.[41] We compared three structural parameters (bite angle, buried volume,[42] and Pd–C(sp^2) bond length) that were expected to have relevance to catalysis across eight different ligands (Table 4).

Scheme 6. General depiction of matched pair analysis.

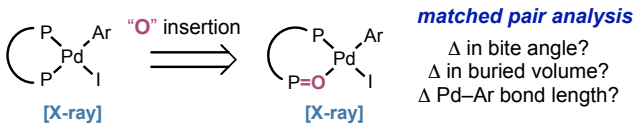

In terms of general considerations, within most of the BPMO oxidative addition complexes in Table 3 (with the exception of those derived from **L20**–**L21**), the BPMO coordinates in a *P,O*-bidentate fashion and the aryl group is situated *trans* to phosphine oxide moiety. For the non-oxidized analogs, the bisphosphine most commonly coordinates in a *P,P*-bidentate mode. Because the bisphosphines included in this study are C_2-symmetric, the remaining coordination sites are sterically and electronically equivalent.

From the matched pair analysis, the Xantphos ligand family stands out as possessing unique coordination behavior that merits comment. Consistent with prior literature,[43] the parent Ph-containing ligand Xantphos (**L12**) is *trans*-*P,P*-chelating as it bisphosphine and becomes *cis*-*P,O*-chelating ligand upon mono-oxidation.[26] We further found that Cy-Xantphos (**L13**) adopts a *P,O,P*-tridentate "pincer-type" coordination mode in the solid state. The Pd center is cationic, and a lone pair of the cyclic ether occupies a coordination site typically held by iodide, rendering it an outer-sphere counteranion. Upon oxidation, in its BPMO form, Cy-Xantphos(O) follows the pattern established for Xantphos(O), adopting a *cis*-*P,O*-chelation mode with inner-sphere iodide.

Table 4: "Matched-pair" analysis between bisphosphine and bisphosphine mono-oxides.

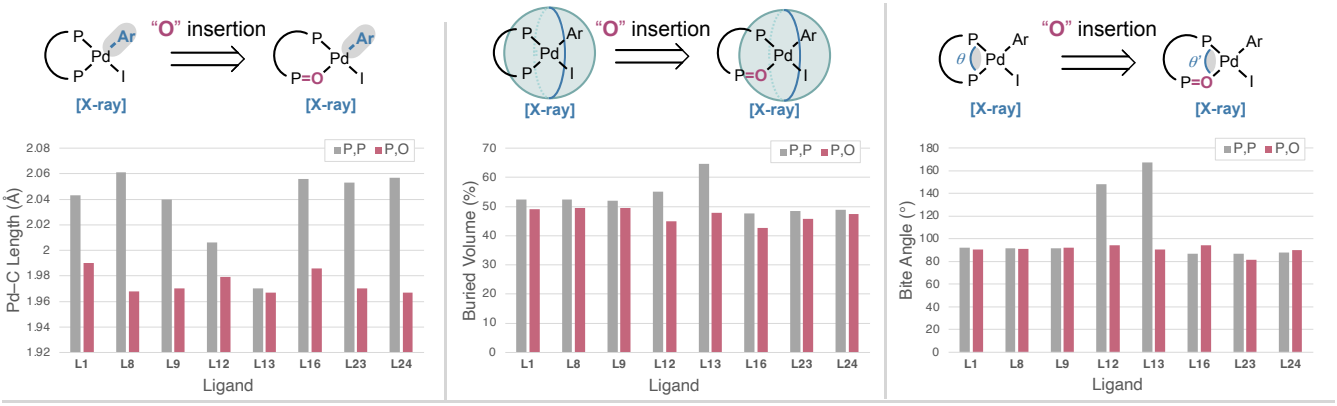

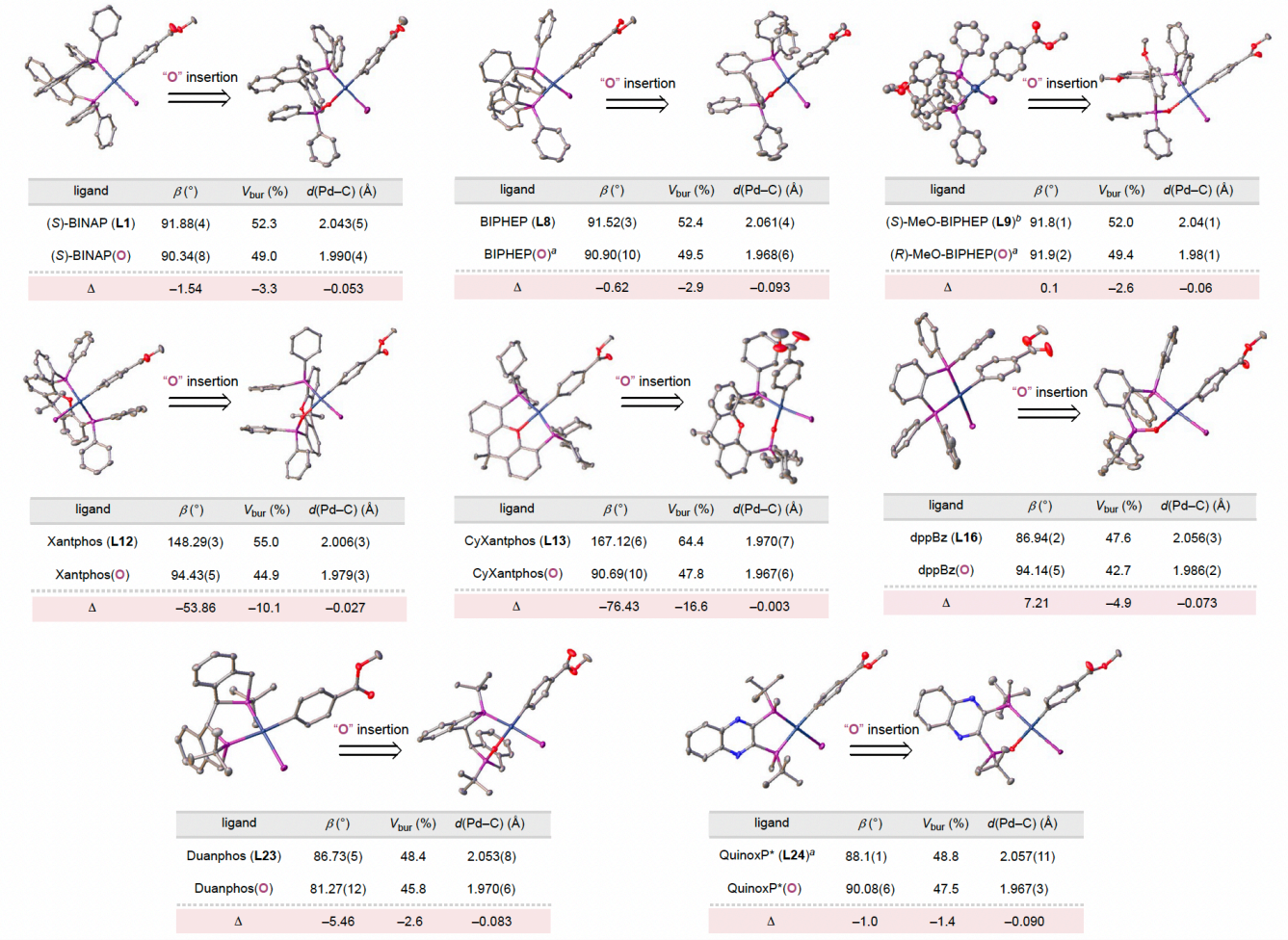

ligand	β (°)	V_{bur} (%)	d(Pd–C) (Å)
(*S*)-BINAP (**L1**)	91.88(4)	52.3	2.043(5)
(*S*)-BINAP(O)	90.34(8)	49.0	1.990(4)
Δ	–1.54	–3.3	–0.053

ligand	β (°)	V_{bur} (%)	d(Pd–C) (Å)
BIPHEP (**L8**)	91.52(3)	52.4	2.061(4)
BIPHEP(O)[a]	90.90(10)	49.5	1.968(6)
Δ	–0.62	–2.9	–0.093

ligand	β (°)	V_{bur} (%)	d(Pd–C) (Å)
(*S*)-MeO-BIPHEP (**L9**)[b]	91.8(1)	52.0	2.04(1)
(*R*)-MeO-BIPHEP(O)[a]	91.9(2)	49.4	1.98(1)
Δ	0.1	–2.6	–0.06

ligand	β (°)	V_{bur} (%)	d(Pd–C) (Å)
Xantphos (**L12**)	148.29(3)	55.0	2.006(3)
Xantphos(O)	94.43(5)	44.9	1.979(3)
Δ	–53.86	–10.1	–0.027

ligand	β (°)	V_{bur} (%)	d(Pd–C) (Å)
CyXantphos (**L13**)	167.12(6)	64.4	1.970(7)
CyXantphos(O)	90.69(10)	47.8	1.967(6)
Δ	–76.43	–16.6	–0.003

ligand	β (°)	V_{bur} (%)	d(Pd–C) (Å)
dppBz (**L16**)	86.94(2)	47.6	2.056(3)
dppBz(O)	94.14(5)	42.7	1.986(2)
Δ	7.21	–4.9	–0.073

ligand	β (°)	V_{bur} (%)	d(Pd–C) (Å)
Duanphos (**L23**)	86.73(5)	48.4	2.053(8)
Duanphos(O)	81.27(12)	45.8	1.970(6)
Δ	–5.46	–2.6	–0.083

ligand	β (°)	V_{bur} (%)	d(Pd–C) (Å)
QuinoxP* (**L24**)[a]	88.1(1)	48.8	2.057(11)
QuinoxP*(O)	90.08(6)	47.5	1.967(3)
Δ	–1.0	–1.4	–0.090

[a] Values represent averages of two independent molecules in the asymmetric unit. [b] Values as described in Ref 41.

Overall, several patterns can be extracted from this analysis. First, both Pd–C(sp^2) bond lengths and buried volumes uniformly decreased upon ligand oxidation. In the case of the Pd–C(sp^2) bond distance, this reflects two factors: (1) a stronger Pd–C(sp^2) bonding interaction with BPMOs compared to bisphosphines due to the metal center being more electron poor and (2) the *trans* influence of the –PR_2(O) group being weaker than the PR_2 group. In the case of buried volume, the decrease in the case of BPMOs compared to bisphophines is due to the steric bulk of the

oxidized phosphine being repositioned one atom further away from the metal center, which pushes steric bulk outside of the 3 Å radius used in the buried volume calculation. On the other hand, there is not a consistent trend of changes of experimentally observed bite angles upon mono-oxidation, likely reflecting the preference of the d^8 metal center to maintain square planar geometry. Here, the largest effects were seen with the wide-bite angle Xantphos family ligands, as discussed above.

Structural Evidence of Hemilability

Most BPMO complexes examined in this study coordinate in a bidentate fashion in the solid state, with the exception of bisphosphine mono-oxides based on 1,1'-ferrocene backbones, where the PR_2=O sidearm dissociates to afford μ-OH dimers.

To gain further insight into hemilability of the bidentate BPMO ligands in Table 3 and its potential importance in catalysis,[24,25] we sought to gain structural evidence of hemilability. We hypothesized that the use of a bidentate κ^2-L,X type ligand may weaken the coordination of the P(V)=O side arm to facilitate dissociation. To this end, the complex Pd^{II}(dppBz(O))(Ar)(I) was treated with Ag(acac), affording the Pd^{II}(dppBz(O))(Ar)(acac) (Scheme 7). The solid-state structure of this complex was studied by X-ray crystallography, and the dppBz(O) was found to coordinate in a monodentate fashion, demonstrating the possibility of both mono- and bidentate coordination modes with dppBz(O) depending on the other ligands coordinated to the metal. Notably, hemilability of dppBz(O) has previously been invoked to rationalize its improved catalytic reactivity compared to dppBz in an intramolecular Heck cyclization.[30]

Scheme 7. Structural comparison between Pd(acac) complexes ligated by dppBz and dppBz(O)

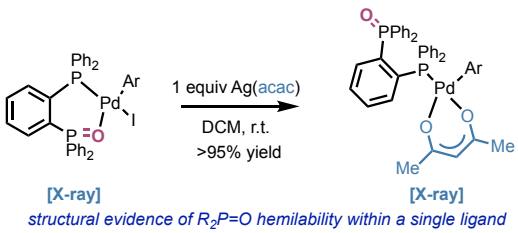

Relative binding strengths of bisphosphine and bisphosphine mono-oxides

Having established the organometallic consequences of bisphosphine ligand oxidation, we next sought to determine relative binding energies of bisphosphines versus BPMOs through DFT calculations supported by experimental observations. To this end, we computed the thermodynamics of ligand exchange reactions between BPMOs and the parent bisphosphines.

In addition to helping rationalize the catalytic performance of a given organopalladium species, we reasoned that this information would be useful in determining the expected catalyst populations under different reaction conditions, particularly in the context of commonly used methods of in situ reduction of Pd^{II} salts to active Pd^0 species with (bis)phosphines, where a >1:1 ligand-to-metal mixture is commonly employed in a catalytic reaction of interest.[44]

For a representative panel of ligands, three organopalladium oxidative addition complexes were considered by DFT (with TPSSh-D3BJ functional): the corresponding Pd^{II}(BPMO)(Ar)(I) (**I**) complex, the putative mixed ligand Pd(BPMO)(bisphosphine)(Ar)(I) intermediate (**II**) and the corresponding Pd^{II}(bisphosphine)(Ar)(I) (**III**) complex (Figure 8A, see Supporting Information for computational details). For 16-electron square-planar d^8 bisphosphine/BPMO oxidative addition complexes, ligand exchange with an incoming bisphosphine presumably proceeds via an associative ligand exchange mechanism that may involve five-coordinate intermediates, but in our analysis the mixed ligand Pd(BPMO)(bisphosphine)(Ar)(I) intermediates (**II**) were found to be lower in energy (see Supporting Information). As expected, DFT computation reveals that the intermediates **II** bearing both bisphosphine and bisphosphine mono-oxide are higher in energy compared to the starting materials in all cases but Xantphos(O), consistent with our findings that these species are therefore not readily observable (Figure 8B). Additionally, the bisphosphine-ligated oxidative addition complexes (**III**) are consistently more stable than BPMO oxidative complexes (**I**) complexes by 4.58–16.18 kcal/mol depending on the ligand employed, suggesting that the former will predominantly coordinate to the metal center with both are present in solution in near-equimolar ratios. Empirical validation of the DFT results was obtained by treating the Pd^{II}(Xantphos(O))(Ar)(I) and Pd^{II}(dppBz(O))(Ar)(I) complexes prepared in Table 3 with the corresponding free bisphosphines and observing quantitative ligand exchange at room temperature in DCM (Figure 8C). The implications of these results in catalysis are discussed in more detail at a later section.

A. ligand exchange reactions considered computationally

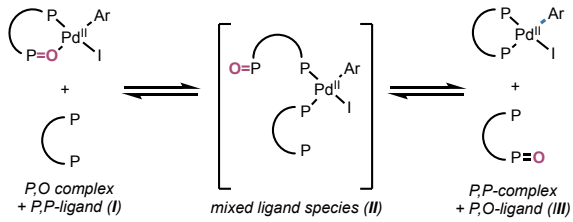

B. computed free energy differences

P,O-complex	P,P-ligand	$\Delta G°_{I\rightarrow II}$ (kcal/mol)	$\Delta G°_{I\rightarrow III}$ (kcal/mol)
BINAP(O)	BINAP (**L1**)	3.93	–11.59
SEGPHOS(O)	SEGPHOS (**L4**)	0.05	–12.50
Xantphos(O)	Xantphos (**L12**)	–1.73	–4.58
dppBz(O)	dppBz (**L16**)	5.17	–16.18

C. experimental validation of ligand exchange equilibria

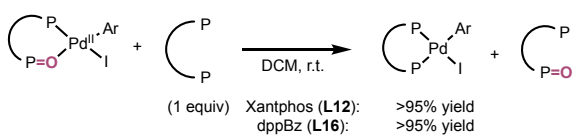

Figure 8. Computational studies of ligand exchange of bisphosphine on Pd^{II}(BPMO) oxidative addition complex. Zero points are defined as starting materials in each of the individual systems studied; TPSSh-D3BJ functional. Ar = 4-(CO_2Me)C_6H_4.

Rationalization of Diagnostic Tests and Broader Implications in Catalysis

The structural and computational data presented above allow more detailed rationalization of the diagnostic test results shown in the preceding section (Scheme 5, Figure 4–8), particularly the Type B and Type C cases in which the oxidation state of the bisphosphine was found to have a profound impact on reaction performance. In the case of the C–N coupling with primary amines (Figure 5), BINAP(O) (**L1**(O)) is an ineffective ligand because the strongly coordinating primary amine outcompetes **L1**(O) for coordination at the metal center, leading to catalyst deactivation. In contrast, the more strongly coordinating bisphosphine ligand BINAP (**L1**) is able to maintain bidentate coordination to the metal, keeping the catalyst on-cycle. In the cases of the C–H activation (Figure 6) and Miyaura borylation reactions (Figure 7), hemilability of the PR_2=O arm of Xantphos(O) (**L12**(O)) is essential for a key step in the catalytic cycle, as it allows coordination of one of the coupling partners (the arene substrate to allow for C–H activation in the case of the former, and the B_2pin_2 reagent to allow for transmetalation in the case of the latter). In both cases, it should also be noted that carboxylate bases employed are capable of adapting both a κ^1 and a κ^2 coordination mode, which creates a low-energy pathway for dissociation of the PR_2=O arm in analogy to the results shown in Scheme 7. Moreover, inhibition of these reactions by addition of non-oxidized Xantphos (**L12**) (1 equiv relative to Pd) (see Figure 7 and Ref. 26) is consistent with the stronger binding of **L12** relative to **L12**(O) (Figure 8B) and the facile nature of ligand exchange (Figure 8C).

The findings of this study have implications beyond the specific catalytic systems demonstrated above in our diagnostic workflow as it pertains to rational selection of precatalysts, ligands, and reaction conditions for widely used coupling reactions (Scheme 8A).

Given that either the BPMO or bisphosphine forms may be the catalytically active species, failure to generate the more active species may result in suboptimal turnover frequency, turnover number, or selectivity, and could be the source of irreproducibility. Unappreciated common pitfalls that we anticipate are depicted in Scheme 8B and C. First, we consider the importance of ligand stoichiometry (Scheme 8B). Excess bisphosphine is commonly used as a sacrificial reductant. If 2 equivalent of ligand relative to a Pd^{II} precatalyst are employed, a theoretical 1:1 mixture of bisphosphine and BPMO would be formed in solution, which will lead to nearly exclusive formation of the *bisphosphine complex* and free BPMO in solution, suppressing any reactivity from a potentially reactive Pd^0(BPMO) species. On the other extreme, insufficient loading of bisphosphine could lead to complete consumption of bisphosphine, which in turn prevents formation of Pd^0(bisphosphine) in solution. Next, we consider the importance of precatalyst and base selection (Scheme 8C.1). The mechanistic studies Scheme 4 and Figures 1–2 point to a decisive role of hydroxide in triggering the key redox reaction between Pd^{II} salts and bisphosphines that leads to BPMO formation. Hence, various Pd^0 precatalysts, such as $Pd_n(dba)_m$ or Pd(COD)(DQ),[45] would not be expected to form BPMOs or form them at a much slower rate. Along these lines, in reactions in which aqueous base is absent, BPMO formation would likely be suppressed. This consideration is especially relevant in a rigorously anhydrous system with organic bases or lipophilic inorganic bases (Scheme 8C.2).[23] Such anhydrous conditions are commonly used for Suzuki–Miyaura reactions involving sensitive coupling partners and in Miyaura borylations to avoid side reactions such protodeboronation and homo-coupling.[46] For instance, in the model Miyaura borylation shown in Figure 7, slow product formation with Pd^{II}(Xantphos)(Ar)(I) as precatalyst can be attributed to the in-situ oxidation of a small amount of Xantphos due to trace amount of water presented in commercial KOPiv (1–2 wt%).[47]

Scheme 8. Broader Implications of this Study

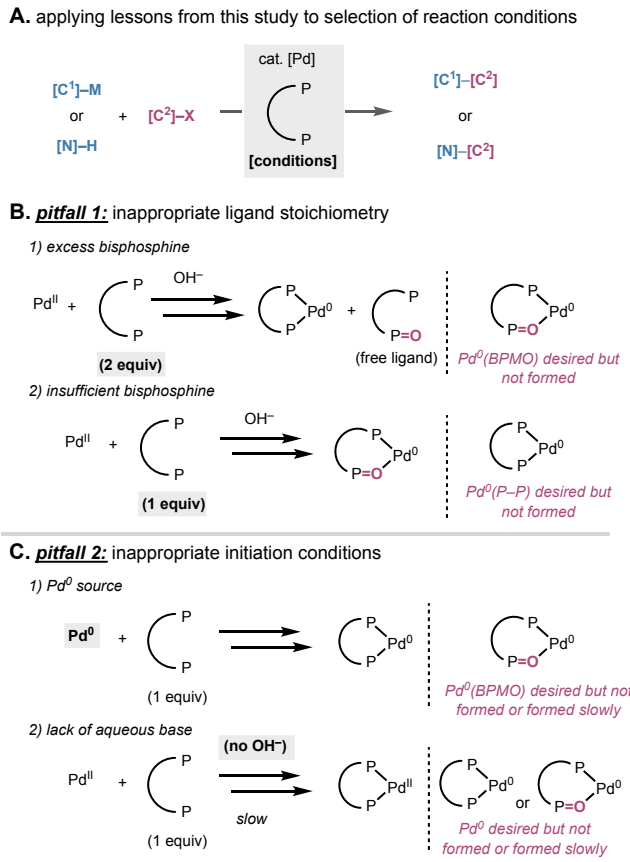

CONCLUSION

The work described herein constitutes a comprehensive study of the redox reaction between Pd^{II} salts and bisphosphines to form Pd(BPMO) complexes and the practical impact of ligand oxidation on select catalytic systems. Through combining organometallic synthesis, reaction kinetics, isotope labeling, structural characterization, and DFT, we provide a detailed examination into bisphosphine ligand oxidation in the

context of precatalyst activation. We hope that this study will serve as a user's guide for the synthesis and catalysis community with utility across wide-ranging catalytic contexts.

ASSOCIATED CONTENT

Supporting Information

The data supporting the findings of this study are available within the article and its Supplementary Information.

AUTHOR INFORMATION

Corresponding Authors

Donna G. Blackmond – Department of Chemistry, The Scripps Research Institute, La Jolla, California 92037, United States; orcid.org/ 0000-0001-9829-8375; Email: blackmond@scripps.edu

Keary M. Engle – Department of Chemistry, The Scripps Research Institute, La Jolla, California 92037, United States; orcid.org/0000-0003-2767-6556; Email: keary@scripps.edu

Authors

Shenghua Yang – Department of Chemistry, The Scripps Research Institute, La Jolla, California 92037, United States

Min Deng – Department of Chemistry, The Scripps Research Institute, La Jolla, California 92037, United States; orcid.org/0000-0002-8256-7240

Ryan A. Daley – Department of Chemistry, The Scripps Research Institute, La Jolla, California 92037, United States

Andrea Darù – Department of Chemistry, The Scripps Research Institute, La Jolla, California 92037, United States orcid.org/0000-0002-0825-2101

William J. Wolf – Chemical Process Development Bris-tol Myers Squibb, New Brunswick, New Jersey 08903, United States; orcid.org/0000-0001-6755-8920

David T. George – Chemical Process Development Bris-tol Myers Squibb, New Brunswick, New Jersey 08903, United States; orcid.org/0000-0002-2926-4144

Senjie Ma – Chemical Process Development Bris-tol Myers Squibb, New Brunswick, New Jersey 08903, United States; orcid.org/0000-0002-7673-1390

Bryn K. Werley – Chemical Process Development Bris-tol Myers Squibb, New Brunswick, New Jersey 08903, United States; orcid.org/0000-0002-8068-6844

Erika Samolova – Department of Chemistry and Biochemistry, University of California, San Diego, La Jolla, California 92093, United States; Institute of Physics of the Czech Academy of Sciences, Na Slovance 2, CZ-182 21 Prague, Czech Republic; orcid.org/0000-0001-9300-8500

Jake Bailey – Department of Chemistry and Biochemistry, University of California, San Diego, La Jolla, California 92093, United States, orcid.org/0000-0002-4659-8189

Milan Gembicky – Department of Chemistry and Biochemistry, University of California, San Diego, La Jolla, California 92093, United States, orcid.org/0000-0002-3898-1612

Jonathan Marshall – Chemical Process Development Bristol Myers Squibb, New Brunswick, New Jersey 08903, United States

Steven R. Wisniewski – Chemical Process Development Bristol Myers Squibb, New Brunswick, New Jersey 08903, United States; orcid.org/0000-0001-6035-4394

Author Contributions

Funding Sources

This work was financially supported by Bristol Myers Squibb.

ACKNOWLEDGMENT

Dr. Laura Pasternack is acknowledged for assistance with NMR analysis. Dr. Prerna Yadav is thanked for preliminary kinetic experiments.

REFERENCE

[1] Shimizu, H.; Nagasaki, I.; Matsumura, K.; Sayo, N.; Saito, T. Developments in Asymmetric Hydrogenation from an Industrial Perspective. *Acc. Chem. Res.* **2007**, *40*, 1385–1393.

[2] Johansson Seechurn, C. C. C.; Kitching, M. O.; Colacot, T. J.; Snieckus, V. Palladium-Catalyzed Cross-Coupling: A Historical Contextual Perspective to the 2010 Nobel Prize. *Angew. Chem. Int. Ed.* **2012**, *51*, 5062–5085.

[3] Ruiz-Castillo, P.; Buchwald, S. L. Applications of Palladium-Catalyzed C–N Cross-Coupling Reactions. *Chem. Rev.* **2016**, *116*, 12564–12649.

[4] Noyori, R.; Takaya, H. BINAP: an efficient chiral element for asymmetric catalysis. *Acc. Chem. Res.* **1990**, *23*, 345–350.

[5] Tang, W.; Zhang, X. New Chiral Phosphorus Ligands for Enantioselective Hydrogenation. *Chem. Rev.* **2003**, *103*, 3029–3070.

[6] Zhang, W.; Chi, Y.; Zhang, X. Developing Chiral Ligands for Asymmetric Hydrogenation. *Acc. Chem. Res.* **2007**, *40*, 1278–1290.

[7] Martin, R.; Buchwald, S. L. Palladium-Catalyzed Suzuki–Miyaura Cross-Coupling Reactions Employing Dialkylbiaryl Phosphine Ligands. *Acc. Chem. Res.* **2008**, *41*, 1461–1473.

[8] Hartwig, J. F. Evolution of a Fourth Generation Catalyst for the Amination and Thioetherification of Aryl Halides. *Acc. Chem. Res.* **2008**, *41*, 1534–1544.

[9] Dang, T. P.; Kagan, H. B. The Asymmetric Synthesis of Hydratropic Acid and Amino-Acids by Homogeneous Catalytic Hydrogenation. *J. Chem. Soc. D* **1971**, 481.

[10] Knowles, W. S. Asymmetric Hydrogenations (Nobel Lecture). *Angew. Chem. Int. Ed.* **2002**, *41*, 1998–2007.

[11] (a) Heck, R. F. New Applications of Palladium in Organic Syntheses. *Pure Appl. Chem.* **1978**, *50*, 691–701. (b) Heck, R. F. Palladium-Catalyzed Reactions of Organic Halides with Olefins. *Acc. Chem. Res.* **2002**, *12*, 146–151.

[12] Hayashi, T.; Konishi, M.; Kumada, M. Dichloro[1,1′-bis(diphenylphosphino)ferrocene]palladium(II): An Effective Catalyst for Cross-Coupling Reaction of a Secondary Alkyl Grignard Reagent with Organic Halides. *Tetrahedron Lett.* **1979**, *20*, 1871–1874.

[13] Sato, Y.; Sodeoka, M.; Shibasaki, M. Catalytic Asymmetric Carbon–Carbon Bond Formation: Asymmetric Synthesis of cis-Decalin Derivatives by Palladium-Catalyzed Cyclization of Prochiral Alkenyl Iodides. *J. Org. Chem.* **1989**, *54*, 4738–4739.

[14] Carpenter, N. E.; Kucera, D. J.; Overman, L. E. Palladium-Catalyzed Polyene Cyclizations of Trienyl Triflates. *J. Org. Chem.* **1989**, *54*, 5846–5848.

[15] Dounay, A. B.; Overman, L. E. The Asymmetric Intramolecular Heck Reaction in Natural Product Total Synthesis. *Chem. Rev.* **2003**, *103*, 2945–2964.

[16] Wolfe, J. P.; Wagaw, S.; Buchwald, S. L. An Improved Catalyst System for Aromatic Carbon–Nitrogen Bond Formation: The Possible Involvement of Bis(Phosphine) Palladium Complexes as Key Intermediates. *J. Am. Chem. Soc.* **1996**, *118*, 7215–7216.

[17] Driver, M. S.; Hartwig, J. F. A Second-Generation Catalyst for Aryl Halide Amination: Mixed Secondary Amines from Aryl Halides and Primary Amines Catalyzed by (DPPF)$PdCl_2$. *J. Am. Chem. Soc.* **1996**, *118*, 7217–7218.

[18] Hamann, B. C.; Hartwig, J. F. Systematic Variation of Bidentate Ligands Used in Aryl Halide Amination. Unexpected Effects of Steric, Electronic, and Geometric Perturbations. *J. Am. Chem. Soc.* **1998**, *120*, 3694–3703.

[19] Bruno, N.; Buchwald, S.; Tudge, M. T. Design and Preparation of New Palladium Precatalysts for C–C and C–N Cross-Coupling Reactions. *Chem. Sci.* **2013**, *4*, 916–920

[20] Amatore, C.; Jutand, A.; M'Barki, M. A. Evidence of the Formation of Serovalent Palladium from $Pd(OAc)_2$ and Triphenylphosphine. *Organometallics* **1992**, *11*, 3009–3013.

[21] Amatore, C.; Carre, E.; Jutand, A.; M'Barki, M. A. Rates and Mechanism of the Formation of Zerovalent Palladium Complexes from Mixtures of $Pd(OAc)_2$ and Tertiary Phosphines and Their Reactivity in Oxidative Additions. *Organometallics* **1995**, *14*, 1818–1826.

[22] Grushin, V. V.; Alper, H. Alkali-Induced Disproportionation of Palladium(II) Tertiary Phosphine Complexes, $[L_2PdCl_2]$, to LO and Palladium(0). Key Intermediates in the Biphasic Carbonylation of ArX Catalyzed by $[L_2PdCl_2]$. *Organometallics* **1993**, *12*, 1890–1901.

[23] Ozawa, F.; Kubo, A.; Hayashi, T. Generation of Tertiary Phosphine-Coordinated Pd(0) Species from $Pd(OAc)_2$ in the Catalytic Heck Reaction. *Chem. Lett.* **1992**, *21*, 2177–2180.

[24] Grushin, V. V. Mixed Phosphine–Phosphine Oxide Ligands. *Chem. Rev.* **2004**, *104*, 1629–1662.

[25] (a) Grushin, V. V. Synthesis of Hemilabile Phosphine–Phosphine Oxide Ligands via the Highly Selective Pd-Catalyzed Mono-oxidation of Bidentate Phosphines: Scope, Limitations, and Mechanism. *Organometallics* **2001**, *20*, 3950–3961. (b) Xue, J.; Zhang, Y.-S.; Huan, Z.; Luo, H.-T.; Dong, L.; Yang, J.-D.; Cheng, J.-P. Phosphonium-Catalyzed Monoreduction of Bisphosphine Dioxides: Origin of Selectivity and Synthetic Applications. *J. Am. Chem. Soc.* **2024**, *146*, 9335–9346.

[26] Ji, Y.; Plata, R. E.; Regens, C. S.; Hay, M.; Schmidt, M.; Razler, T.; Qiu, Y.; Geng, P.; Hsiao, Y.; Rosner, T.; Eastgate, M. D.; Blackmond, D. G. Mono-Oxidation of Bidentate Bis-phosphines in Catalyst Activation: Kinetic and Mechanistic Studies of a Pd/Xantphos-Catalyzed C–H Functionalization. *J. Am. Chem. Soc.* **2015**, *137*, 13272–13281.

[27] Li, H.; Belyk, K. M.; Yin, J.; Chen, Q.; Hyde, A.; Ji, Y.; Oliver, S.; Tudge, M. T.; Campeau, L.-C.; Campos, K. R. Enantioselective Synthesis of Hemiaminals via Pd-Catalyzed C–N Coupling with Chiral Bisphosphine Mono-oxides. *J. Am. Chem. Soc.* **2015**, *137*, 13728–13731.

[28] Ji, Y.; Li, H.; Hyde, A. M.; Chen, Q.; Belyk, K. M.; Lexa, K. W.; Yin, J.; Sherer, E. C.; Williamson, R. T.; Brunskill, A.; Ren, S.; Campeau, L.-C.; Davies, I. W.; Ruck, R. T. A Rational Pre-Catalyst Design for Bis-Phosphine Mono-Oxide Palladium Catalyzed Reactions. *Chem. Sci.* **2017**, *8*, 2841–2851.

[29] Moore, M. J.; Qu, S.; Tan, C.; Cai, Y.; Mogi, Y.; Jamin Keith, D.; Boger, D. L. Next-Generation Total Synthesis of Vancomycin. *J. Am. Chem. Soc.* **2020**, *142*, 16039–16050.

[30] Cadena, M.; Villatoro, R. S.; Gupta, J. S.; Phillips, C.; Allen, J. B.; Arman, H. D.; Wherritt, D. J.; Clanton, N. A.; Ruchelman, A. L.; Simmons, E. M.; DelMonte, A. J.; Coombs, J. R.; Frantz, D. E. Pd-Catalyzed Chemoselective *O*-Benzylation of Ambident 2-Quinolinone Nucleophiles. *ACS Catal.* **2022**, *12*, 10199–10206.

[31] Doggett, A.; Hay, M.; McKenna, S.; Saurer, E. M.; Steinhardt, S.; Tan, Y.; Wilbert, C. R.; Wisniewski, S. R. Development of a Chromane-Forming Heck Reaction: Bisphosphine Mono-Oxide Mediated Regioselectivity Perturbed by Solvent-Based Peroxide Formation. *Org. Process Res. Dev.* **2023**, *27*, 1129–1135.

[32] Murray, J. I.; Zhang, L.; Simon, A.; Silva Elipe, M. V.; Wei, C. S.; Caille, S.; Parsons, A. T. Kinetic and Mechanistic Investigations to Enable a Key Suzuki Coupling for Sotorasib Manufacture—What a Difference a Base Makes. *Org. Process Res. Dev.* **2023**, *27*, 198–205

[33] Ingoglia, B. T.; Buchwald, S. L. Oxidative Addition Complexes as Precatalysts for Cross-Coupling Reactions Requiring Extremely Bulky Biarylphosphine Ligands. *Org. Lett.* **2017**, *19*, 2853–2856.

[34] For example, in the case of **L1(O)**, the oxidative addition complex with 4-CO_2Me-C_6H_4I readily precipitated from the reaction medium.

[35] Xie, J.-H.; Zhou, Q.-L. Chiral Diphosphine and Monodentate Phosphorus Ligands on a Spiro Scaffold for Transition-Metal-Catalyzed Asymmetric Reactions. *Acc. Chem. Res.* **2008**, *41*, 581–593

[36] Hu, J.; Hirao, H.; Li, Y.; Zhou, J. Palladium-Catalyzed Asymmetric Intermolecular Cyclization. *Angew. Chem. Int. Ed.* **2013**, *52*, 8676–8680.

[37] Wu, C.; Zhou, J. Asymmetric Intermolecular Heck Reaction of Aryl Halides. *J. Am. Chem. Soc.* **2014**, *136*, 650–652.

[38] (a) Singh, U. K.; Strieter, E. R.; Blackmond, D. G.; Buchwald, S. L. Mechanistic Insights into the Pd(BINAP)-Catalyzed Amination of Aryl Bromides: Kinetic Studies under Synthetically

Relevant Conditions. *J. Am. Chem. Soc.* **2002**, *124*, 14104–14114. (b) Shekhar, S.; Ryberg, P.; Hartwig, J. F.; Mathew, J. S.; Blackmond, D. G.; Strieter, E. R.; Buchwald, S. L. Reevaluation of the Mechanism of the Amination of Aryl Halides Catalyzed by BINAP-Ligated Palladium Complexes. *J. Am. Chem. Soc.* **2006**, *128*, 3584–3591. (c) Schmidt, O. P.; Blackmond, D. G. Temperature-Scanning Reaction Protocol Offers Insights into Activation Parameters in the Buchwald–Hartwig Pd-Catalyzed Amination of Aryl Halides. *ACS Catal.* **2020**, *10*, 8926–8932.

[39]] It should be noted that use of iodide-containing oxidative addition complexes as precatalysts has the potential to introduce complications in C–N cross-coupling reactions due to documented iodide inhibition effects: Fors, B. P.; Davis, N. R.; Buchwald, S. L. An Efficient Process for Pd-Catalyzed C–N Cross-Coupling Reactions of Aryl Iodides: Insight Into Controlling Factors. *J. Am. Chem. Soc.* **2009**, *131*, 5766–5768.

[40] Primer, D. N.; Yong, K.; Ramirez, A.; Kreilein, M.; Ferretti, A. C.; Ruda, A. M.; Fleary-Roberts, N.; Moseley, J. D.; Forsyth, S. M.; Evans, G. R.; Traverse, J. F. Development of a Process to a 4-Arylated 2-Methylisoquinolin-1(2*H*)-one for the Treatment of Solid Tumors: Lessons in Ortho-Bromination, Selective Solubility, Pd Deactivation, and Form Control. *Org. Process Res. Dev.* **2022**, *26*, 1458–1469.

[41] Tschoerner, M.; Pregosin, P. S.; Albinati, A. Contributions to the Enantioselective Heck Reaction Using MeO–Biphep Ligands. The Case Against Dibenzylidene Acetone. *Organometallics* **1999**, *18*, 670–678.

[42] Falivene, L.; Cao, Z.; Petta, A.; Serra, L.; Poater, A.; Oliva, R.; Scarano, V.; Cavallo, L. Towards the Online Computer-Aided Design of Catalytic Pockets. *Nat. Chem.* **2019**, *11*, 872–879.

[43] Yin, J.; Buchwald, S. L. Pd-Catalyzed Intermolecular Amidation of Aryl Halides: The Discovery that Xantphos Can Be Trans-Chelating in a Palladium Complex. *J. Am. Chem. Soc.* **2002**, *124*, 6043-6048

[44] For representative examples, see: (a) Amatore, C.; Jutand, A.; Thuilliez, A. Formation of Palladium(0) Complexes from Pd(OAc)2 and a Bidentate Phosphine Ligand (dppp) and Their Reactivity in Oxidative Addition. *Organometallics* **2001**, *20*, 3241–3249. (b) Fors, B. P.; Krattiger, P.; Strieter, E.; Buchwald, S. L. Water-Mediated Catalyst Preactivation: An Efficient Protocol for C–N Cross-Coupling Reactions. *Org. Lett.* **2008**, *10*, 3505–3508. (c) Wei, C. S.; Davies, G. H. M.; Soltani, O.; Albrecht, J.; Gao, Q.; Pathirana, C.; Hsiao, Y.; Tummala, S.; Eastgate, M. D. The Impact of Palladium(II) Reduction Pathways on the Structure and Activity of Palladium(0) Catalysts. *Angew. Chem. Int. Ed.* **2013**, *52*, 5822–5826.

[45] He, W.-J.; Qin, W.-Z.; Yang, S.; Ma, S.; Kim, S.; Schultz, J. E.; Palkowitz, M. D.; He, C.; Ma, A.; Schmidt, M. A.; Gembicky, M.; Wisniewski, S. R.; Engle, K. M. Pd(COD)(DQ): A Stable, Versatile, and Monometallic Palladium(0) Source for Organometallic Synthesis and Catalysis. *ChemRxiv* **2024**, DOI: 10.26434/chemrxiv-2024-sj081.

[46] a) Barder, T. E.; Walker, S. D.; Martinelli, J. R.; Buchwald, S. L. Catalysts for Suzuki–Miyaura Coupling Processes: Scope and Studies of the Effect of Ligand Structure. *J. Am. Chem. Soc.* **2005**, *127*, 4685–4696. b) Gillis, E. P.; Burke, M. D. A Simple and Modular Strategy for Small Molecule Synthesis:‚Ää Iterative Suzuki‚àíMiyaura Coupling of B-Protected Haloboronic Acid Building Blocks. *J. Am. Chem. Soc.* **2007**, *129*, 6716–6717. c) Kassel, V. M.; Hanneman, C. M.; Delaney, C. P.; Denmark, S. E. Heteroaryl–Heteroaryl, Suzuki–Miyaura, Anhydrous Cross-Coupling Reactions Enabled by Trimethyl Borate. *J. Am. Chem. Soc.* **2021**, *143*, 13845–13853.

[47] Commercial lots of KOPiv from different vendors were analyzed by Karl Fischer titration.